

Langevin PDF simulation of particle deposition in a turbulent pipe flow

Sergio Chibbaro¹, Jean-Pierre Minier²

¹ Dept. of Mechanical Engineering, University of “Tor Vergata”,

Viale Politecnico, Rome, Italy

chibbaro@iac.cnr.it

²Electricité de France, Div. R&D, MFEE,

6 Quai Watier, 78400 Chatou, France

E-mail: Jean-Pierre.Minier@edf.fr

Abstract

The paper deals with the description of particle deposition on walls from a turbulent flow over a large range of particle diameter, using a Langevin PDF model. The first aim of the work is to test how the present Langevin model is able to describe this phenomenon and to outline the physical aspects which play a major role in particle deposition. The general features and characteristics of the present stochastic model are first recalled. Then, results obtained with the standard form of the model are presented along with an analysis which has been carried out to check the sensitivity of the predictions on different mean fluid quantities. These results show that the physical representation of the near-wall physics has to be improved and that, in particular, one possible route is to introduce specific features related to the near-wall coherent structures. In the following, we propose a simple phenomenological model that introduces some of the effects due to the presence of turbulent coherent structures on particles in a thin layer close to the wall. The results obtained with this phenomenological model are in good agreement with ex-

perimental evidence and this suggests to pursue in that direction, towards the development of more general and rigorous stochastic models that provide a link between a geometrical description of turbulent flow and a statistical one.

I. INTRODUCTION

Particle deposition from a turbulent flow on walls is an important phenomenon which is observed in many engineering applications, for example thermal and nuclear systems, cyclone separators, spray cooling and which is also present in various environmental situations. Given the large number of possible applications, a lot of interest has been devoted to this subject and many studies have been carried out in the last decades.

Different experiments have been conducted to observe deposition in turbulent flows. In most of them, attention is focused on the deposition velocity^{1,2} which is defined as $k_p = m_p/\bar{C}$, where m_p is the mass flux and \bar{C} is the bulk mean particle concentration. This deposition rate, often presented as the dimensionless deposition velocity k_p/u^* , is a function of the dimensionless particle relaxation time, τ_p^+ defined as

$$\tau_p^+ = S^+ \frac{u^*}{U_{p0}} = \frac{d_p^2 \rho_p U_{p0} u^*}{18 \mu_f \nu_f} \frac{u^*}{U_{p0}} = \frac{d_p^2 \rho_f^2 u^{*2}}{18 \mu_f^2} \frac{\rho_p}{\rho_f} \quad (1)$$

where S^+ is the dimensionless stopping distance, U_{p0} is the particle initial velocity and u^* the friction velocity. In this work, u^* has been computed with the Blasius formula, $u^* = [0.03955 Re^{0.25}]^{0.5} U_m$, with U_m the bulk mean velocity. The deposition velocity is indeed the key point in many engineering applications where the interest is to obtain the curve that gives k_p/u^* as a function of τ_p^+ , that is as a function of the particle diameter. Recently, several experimental studies and DNS studies of particle deposition have been presented^{3–16} and have improved the understanding of the physical mechanisms at play. In particular, much information has been obtained about the dynamical structures of wall-bounded flows, such as the coherent structures which manifest themselves in the near-wall region. It is largely accepted that particle transfer in the wall region and also deposition

onto walls are processes dominated by near-wall turbulent coherent structures (sweeps and ejections), which are instantaneous realizations of the Reynolds stresses, and that particles tend to remain trapped along the streaks when in the viscous-layer^{3–5,8,11}. However, the importance of these mechanisms for particle deposition depends on particle inertia. In a somewhat crude picture, light particles follow closely sweeps and ejections and their motion towards the wall appears to be very well correlated with turbulent structures. Therefore, they are found to deposit mainly with negligible wall-normal velocities and large near-wall residence time. This mechanism of deposition has been called *diffusional*¹³. On the contrary, heavy particles are not so well correlated with turbulent structures and their motion is less influenced by them in the near-wall region. Therefore, heavy particles deposit with large wall-normal velocities and small near-wall residence time, that is by the so-called *free-flight* mechanism^{10,13}.

Considering the engineering importance of the subject, models that reach acceptable compromise between simplicity and accuracy are needed. While DNS calculations may be regarded as numerical experiments and give access to the complete picture, they remain limited to simple geometries and low-Reynolds number flows. Therefore, a statistical approach is still necessary to describe the motion of particles in a turbulent flow. Within this framework, and since the objective is to simulate the entire curve of the deposition velocity for a whole range of particle inertia or diameter, a Lagrangian approach appears appropriate. Indeed, in this approach, the trajectories of individual particles are tracked and polydispersion is treated without approximation. The influence of the underlying turbulent fluid is represented, in the particle equation of motion, by stochastic models. Many of the Lagrangian models proposed today belong to the class of the so-called *random-walk* models^{17–19}, which define the velocity as the sum of the local mean fluid velocity and a random fluctuating velocity sampled from a Gaussian distribution. Unfortunately, these models can suffer from problems of consistency, in particular the so-called spurious drift effect. This is important for particle deposition, since one has to simulate the behavior of very small particles which nearly represent fluid tracers. In the present paper, we use a Langevin model²¹ in which

the velocity of the fluid seen by particles is simulated by a diffusion stochastic process. This model is consistent in the tracer limit by construction, and is thus free of spurious drifts^{20,17}. Furthermore, the model is formulated in terms of instantaneous variables which allows a direct introduction of external information provided by fundamental studies (DNS, experiments).

The present numerical Langevin model is applied to a case of particle deposition in a turbulent pipe-flow. A first purpose is to analyze how the present form of the Langevin model performs for particle deposition. A second purpose is to bring out the modeling points that are important in this situation so that directions of improvement are clearly indicated. In particular, a new phenomenological model which takes into account some aspects due to the presence of near-wall instantaneous coherent structures will be proposed. In this way, we propose a first link between a statistical model, such as the present Langevin model, and some geometrical features recently found out by DNS analysis^{11–14}. The goal of the work is therefore to propose simple and phenomenological models and, also, to indicate whether introducing geometrical features in a Lagrangian stochastic approach can be useful for particle deposition simulations. This approach has some analogy with the analysis carried out by Pope and Yeung some years ago for the single-phase fluid stochastic modeling¹⁵.

The paper is divided as follows. In section II, we present the Langevin model that will be used throughout the work. In section III, we present the test-case that will be studied. Results obtained with the standard form of the PDF model are discussed and a new phenomenological model for the effect of near-wall structures is proposed. Finally, conclusions are proposed.

II. LANGEVIN MODEL

In this section we recall briefly the theoretical background of turbulent two-phase flows and we present the Langevin stochastic model which will be referred to as the standard model and which will be used in following numerical investigations. The modeling starting point

is the exact equations of motion. Since two different phases are present, the continuous one and the discrete dispersed one, the complete problem is described by two sets of equations. The continuous phase is described by the Navier-Stokes equations:

$$\frac{\partial U_{f,j}}{\partial x_j} = 0, \quad (2a)$$

$$\frac{\partial U_{f,i}}{\partial t} + U_{f,j} \frac{\partial U_{f,i}}{\partial x_j} = -\frac{1}{\rho_f} \frac{\partial P}{\partial x_i} + \nu \frac{\partial^2 U_{f,i}}{\partial x_j^2}, \quad (2b)$$

while the discrete particle equations in the limit $\rho_p \gg \rho_f$ are^{22,23}

$$\frac{d\mathbf{x}_p}{dt} = \mathbf{U}_p, \quad (3a)$$

$$\frac{d\mathbf{U}_p}{dt} = \frac{1}{\tau_p} (\mathbf{U}_s - \mathbf{U}_p) + \mathbf{g}, \quad (3b)$$

where $\mathbf{U}_s = \mathbf{U}(\mathbf{x}_p(\mathbf{t}), \mathbf{t})$ is the fluid velocity seen, *i.e.* the fluid velocity sampled along the particle trajectory $\mathbf{x}_p(\mathbf{t})$, not to be confused with the fluid velocity $\mathbf{U}_f = \mathbf{U}(\mathbf{x}_f(\mathbf{t}), \mathbf{t})$ denoted with the subscript f . The particle relaxation time is defined as

$$\tau_p = \frac{\rho_p}{\rho_f} \frac{4d_p}{3C_D |\mathbf{U}_r|}, \quad (4)$$

where the local instantaneous relative velocity is $\mathbf{U}_r = \mathbf{U}_s - \mathbf{U}_p$ and the drag coefficient C_D is a non-linear function of the particle-based Reynolds number, $Re_p = d_p |\mathbf{U}_r| / \nu_f$, which means that C_D is a complicated function of the particle diameter d_p , Clift *et al.*²⁴. For example, a very often retained empirical form for the drag coefficient is

$$C_D = \begin{cases} \frac{24}{Re_p} [1 + 0.15 Re_p^{0.687}] & \text{if } Re_p \leq 1000, \\ 0.44 & \text{if } Re_p \geq 1000. \end{cases} \quad (5)$$

In many papers the Saffman lift force has been considered although, strictly speaking, this lift force is only valid in an infinite domain and, therefore, should not be considered in the vicinity of a wall. With respect to the issue of lift forces, the situation remains rather complex since quite a variety of different expressions have been put forward, each time for different particle and flow descriptions, and it is difficult to gather which ones are relevant or even whether they correspond to different lift forces or to different expressions of the same

lift force. Yet, recently an “optimal” lift force, based on rigorous studies^{6,25–27}, has been proposed and seems to have helped to clarify the situation. This expression has been used in a careful numerical LES simulation²⁸ to test its importance for particle deposition and numerical outcomes have showed only a slight reduction in the deposition rate and mainly in the range of small diameters. For these reasons, the lift force has not been included in the present study.

In some approaches, other forces are also included, namely thermophoretic and electrostatic forces^{19,29}. Nevertheless, thermophoretic forces are important only for ultrafine particles in presence of a temperature gradient²⁹ and thus are neglected in the present paper, since the fluid temperature is considered uniform. Furthermore, electrostatic forces have a range of action so small that they can be important only for particles with a diameter smaller than one micron³⁰ and, thus, they are not considered in the present paper, since only particles with a larger size are analysed. Indeed, it may be quite possible to include in the particle equation of motion a rather complete chemical force between particles and the wall, given for example by the classical DLVO theory that includes Van der Waals forces as well as electrostatic attractive or repulsive forces³¹. This force is important mainly in a very thin layer close to the wall for very small, or colloidal, particles. This expression has not been retained also because, in the present approach, we have chosen to concentrate mainly on the hydrodynamical effects on particle deposition. Thus, a simplified chemical force is actually used : there is no chemical force inside the flow domain but when a particle hits the wall it is regarded as being deposited, that is an infinite adhesion force is assumed.

In two-phase flow modeling, various approaches can be followed. In this paper, we have chosen an hybrid Eulerian/Lagrangian PDF one. We describe the continuous phase with a classical Eulerian momentum approach, that is the fluid phase is represented by Reynolds average Navier-Stokes (RANS) equations. On the other hand, the particle phase is solved with a PDF approach where we substitute the instantaneous exact equations with a set of modeled instantaneous equations. From a mathematical point of view, these modeled equations are Langevin equations, that is a set of stochastic differential equations (SDEs).

A complete and rigorous presentation of this approach can be found elsewhere^{21,32} while for a general presentation of the argument of PDF modeling in turbulence we refer to a classical reference³³ and to the recent book of Pope³⁴. The Langevin model discussed in this paper was recently proposed²¹ and has the form

$$dx_{p,i} = U_{p,i} dt \quad (6)$$

$$dU_{p,i} = \frac{1}{\tau_p} (U_{s,i} - U_{p,i}) dt \quad (7)$$

$$\begin{aligned} dU_{s,i} = & -\frac{1}{\rho_f} \frac{\partial \langle P \rangle}{\partial x_i} dt + (\langle U_{p,j} \rangle - \langle U_{f,j} \rangle) \frac{\partial \langle U_{f,i} \rangle}{\partial x_j} dt \\ & - \frac{1}{T_{L,i}^*} (U_{s,i} - \langle U_{f,i} \rangle) dt \\ & + \sqrt{\langle \epsilon \rangle \left(C_0 b_i \tilde{k}/k + \frac{2}{3} (b_i \tilde{k}/k - 1) \right)} dW_i. \end{aligned} \quad (8)$$

The crossing-trajectory effect (CTE), that is the effect due to the presence of external forces, has been modeled with the introduction of modified time-scales according to Csanady's analysis. Assuming for the sake of simplicity that the mean drift is aligned with the first coordinate axis, the modeled expressions for the timescales are, in the longitudinal direction:

$$T_{L,1}^* = \frac{T_L}{\sqrt{1 + \beta^2 \frac{\langle \mathbf{U}_r \rangle^2}{2k/3}}} \quad (9)$$

and in the transverse directions (axis labeled 2 and 3)

$$T_{L,2}^* = T_{L,3}^* = \frac{T_L}{\sqrt{1 + 4\beta^2 \frac{\langle \mathbf{U}_r \rangle^2}{2k/3}}} \quad (10)$$

where T_L represents the Lagrangian time-scale of velocity correlations and it is defined by

$$T_L = \frac{1}{(1/2 + 3/4 C_0)} \frac{k}{\langle \epsilon \rangle}, \quad (11)$$

in which β is the ratio of the Lagrangian and the Eulerian timescales of the fluid $\beta = T_L/T_E$, that is considered as a constant. In the diffusion matrix we have introduced a new kinetic

energy:

$$b_i = \frac{T_L}{T_{L,i}^*} ; \quad \tilde{k} = \frac{3 \sum_{i=1}^3 b_i \langle u_{f,i}^2 \rangle}{2 \sum_{i=1}^3 b_i}. \quad (12)$$

All these expressions are to be regarded as being local in space and evaluated at the particle position, that is for example $T_L = T_L(\mathbf{x}_p)$, which shows that, in nonhomogeneous situations, the stochastic equations are non-linear. The reasoning leading to the construction of this Langevin model as well as a discussion of the case of general axis direction are developped in another work³².

It is important to underline that the solution of this set of stochastic equations represents a Monte Carlo simulation of the underlying pdf. Therefore, this approach is equivalent to solving directly the corresponding equation for the pdf in the state-variable space. Indeed, the complete Langevin equation model for the state vector $\mathbf{Z} = (\mathbf{x}_p, \mathbf{U}_p, \mathbf{U}_s)$ can be written

$$dx_{p,i} = U_{p,i} dt \quad (13a)$$

$$dU_{p,i} = A_{p,i}(t, \mathbf{Z}) dt \quad (13b)$$

$$dU_{s,i} = A_{s,i}(t, \mathbf{Z}) dt + B_{s,ij}(t, \mathbf{Z}) dW_j. \quad (13c)$$

This formulation is equivalent to a Fokker-Planck equation given in closed form for the corresponding pdf $p_p^L(t; \mathbf{y}_p, \mathbf{V}_p, \mathbf{V}_s)$ which is, in sample space

$$\frac{\partial p_p^L}{\partial t} + V_{p,i} \frac{\partial p_p^L}{\partial y_{p,i}} = - \frac{\partial}{\partial V_{p,i}} (A_{p,i} p_p^L) - \frac{\partial}{\partial V_{s,i}} (A_{s,i} p_p^L) + \frac{1}{2} \frac{\partial^2}{\partial V_{s,i} \partial V_{s,j}} ([\mathbf{B}_s \mathbf{B}_s^T]_{ij} p_p^L) . \quad (14)$$

It can then be shown that the Eulerian MDF (mass density function) $F_p^E(t, \mathbf{x}; \mathbf{V}_p, \mathbf{V}_s)$ satisfies the same equation from which the resulting (Eulerian) mean field equations can be computed³².

Some specific characteristics of the present Langevin type of model are worth emphasizing, particularly with respect to the simulation of small-inertia particles using an hybrid formulation. Indeed, for very small particles (for which the mean relative drift can be seen as negligible $\langle \mathbf{U}_r \rangle \simeq 0$) corresponding to the limit of vanishing inertia, $\tau_p \rightarrow 0$, also called the particle-tracer limit), the model reverts to a Langevin model for a fluid particle since

$\mathbf{U}_p \rightarrow \mathbf{U}_f$ and has the form :

$$dx_{f,i} = U_{f,i} dt \quad (15a)$$

$$dU_{f,i} = -\frac{1}{\rho} \frac{\partial \langle P \rangle}{\partial x_i} dt - \frac{1}{T_L} (U_i - \langle U_i \rangle) dt + \sqrt{C_0 \langle \epsilon \rangle} dW_i. \quad (15b)$$

This model corresponds to the Simplified Langevin Model (SLM)³³.

A first important issue to consider is to be sure that the model is free of spurious drifts. In models such as SLM, which are written as stochastic differential equations for the instantaneous fluid velocity \mathbf{U}_f , spurious drifts (which are related to spurious accumulations of fluid particles in regions of low turbulent kinetic energy) are naturally avoided with the proper introduction of the mean-pressure gradient^{20,32}. To underline that point, it may useful to rewrite the same model for the fluid particle velocity fluctuating component $\mathbf{u}_f = \mathbf{U}_f - \langle \mathbf{U}_f \rangle$ which is

$$dx_{f,i} = (\langle U_{f,i} \rangle + u_{f,i}) dt \quad (16a)$$

$$du_{f,i} = \frac{\partial \langle u_{f,i} u_{f,k} \rangle}{\partial x_k} dt - u_{f,k} \frac{\partial \langle U_{f,i} \rangle}{\partial x_k} dt - \frac{u_{f,i}}{T_L} dt + \sqrt{C_0 \langle \epsilon \rangle} dW_i. \quad (16b)$$

Thus, in non-homogeneous situations, the increments of the fluctuating velocity components along a Lagrangian trajectory have a non-zero value, due to the first term on the rhs of the last equation (there is an underlying difference between means taken along fluid particle trajectory, in a Lagrangian setting, and mean values at a fixed point, in an Eulerian setting, which for the fluctuating velocity is of course zero). Although surprising at first sight, this term is absolutely necessary so as to be able to respect the incompressibility constraint which states that a uniform fluid particle concentration should remain uniform even in a non-homogeneous situation^{17,20,32}. However, models (for example some models of the random-walk type) that simply add to the mean fluid velocity a fluctuating component that has a zero-mean value (thus confusing Lagrangian and Eulerian averaging operators) are equivalent to models where an artificial drift velocity is implicitly added in the correct equation, namely $v_{d,i} = -\partial \langle u_{f,i} u_{f,k} \rangle / \partial x_k$. In the channel flow approximation, where $v_d = -d \langle v^2 \rangle / dy$ in the direction normal to the wall, this amounts to adding a spurious drift that artificially

drives fluid particle away from the wall, thereby reducing the possibility of small-particle deposition.

A second relevant issue is the consistency of Eulerian and Lagrangian turbulence modeling. Indeed, in terms of Eulerian mean equations, the SLM model is equivalent to the following set of equations³⁵ :

$$\frac{\partial \langle U_i \rangle}{\partial x_i} = 0 \quad (17)$$

$$\frac{\partial \langle U_i \rangle}{\partial t} + \langle U_j \rangle \frac{\partial \langle U_i \rangle}{\partial x_j} + \frac{\partial \langle u_i u_j \rangle}{\partial x_j} = -\frac{1}{\rho} \frac{\partial \langle P \rangle}{\partial x_i} \quad (18)$$

$$\begin{aligned} \frac{\partial \langle u_i u_j \rangle}{\partial t} + \langle U_k \rangle \frac{\partial \langle u_i u_j \rangle}{\partial x_k} + \frac{\partial \langle u_i u_j u_k \rangle}{\partial x_k} = & -\langle u_i u_k \rangle \frac{\partial \langle U_j \rangle}{\partial x_k} - \langle u_j u_k \rangle \frac{\partial \langle U_i \rangle}{\partial x_k} \\ & -\frac{2}{T_L} \langle u_i u_j \rangle + C_0 \langle \epsilon \rangle \delta_{ij}. \end{aligned} \quad (19)$$

Using the expression retained for T_L in Eq. (11), the transport equation for the second-order moments can be re-expressed as :

$$\begin{aligned} \frac{\partial \langle u_i u_j \rangle}{\partial t} + \langle U_k \rangle \frac{\partial \langle u_i u_j \rangle}{\partial x_k} + \frac{\partial \langle u_i u_j u_k \rangle}{\partial x_k} = & -\langle u_i u_k \rangle \frac{\partial \langle U_j \rangle}{\partial x_k} - \langle u_j u_k \rangle \frac{\partial \langle U_i \rangle}{\partial x_k} \\ & -(1 + \frac{3}{2} C_0) \left(\langle u_i u_j \rangle - \frac{2}{3} k \delta_{ij} \right) - \frac{2}{3} \delta_{ij} \langle \epsilon \rangle. \end{aligned} \quad (20)$$

This shows that the SLM corresponds to a $R_{ij} - \epsilon$ Rotta model³⁵. It is important to underline that the complete stochastic model, which is based on an assumption of an isotropic return-to-equilibrium term for the closure of the pressure-strain correlation, is not isotropic even in the asymptotic case of tracer particles, that is for the fluid case. Yet, as it transpires from its name, the SLM is perhaps the simplest possible stochastic model consistent with classical Reynolds-stress second-order modeling and its capacity to reproduce high anisotropy, such as in the near-wall turbulent boundary layer, is limited³⁶. It is possible to replace the simple return-to-equilibrium term in Eq. (15b) by a more general matrix G_{ij} which is a function of local fluid mean velocity gradients^{35,36} so as to retrieve more complex Reynolds-stress models for $\langle u_i u_j \rangle$ which may improve numerical predictions in highly-anisotropic regions. New complete (and more complex) Langevin models have also been recently put forward with down-to-the-wall integration and are able to reproduce the high-anisotropy of the Reynolds-

stress quite well³⁷. However, in the present context, we are using an hybrid formulation and we believe that, before resorting to more involved models, it is important to stress the consistency issue. Indeed, in such a formulation, one turbulence model is used in the Eulerian part for the prediction of the fluid mean fields such as the mean velocity and Reynolds-stress. These fluid mean fields are provided to the Lagrangian solver in Eqs. (6)-(8) which also corresponds to a turbulence model, as it was just underlined. For small-inertia particle, we have therefore a duplicate turbulence model and it is very important to ensure that these two turbulence models be as consistent as possible^{34,38}. Indeed, it has been shown that to couple models which correspond to different turbulence models (for instance DNS and the present Lagrangian model) may introduce some inconsistencies at the level of particle equations and, thus, may lead to unphysical results in particular for the numerical prediction of wall-normal stress, say $\langle v^2 \rangle$, which is important if we are to simulate particle fluxes towards the walls^{38,39}. Therefore, as a first step, we have retained a simple version, namely the SLM model, which is consistent with usual Reynolds-stress models as a kind of sound basis for the numerical investigations on particle deposition though it is clear that, at least for the prediction of fluid mean quantities, this leaves room for improvement by using more complex Langevin ideas.

III. NUMERICAL RESULTS

In this section, we present numerical results for the deposition of particles in a vertical pipe flow at a Reynolds number of 10 000, which corresponds to the experiment of Liu and Agarwal (1974)¹.

In order to describe the particle phase, 10,000 individual particles (920 kg/m^3 in density) of 10 diameters ($1.4 - 68.5 \mu\text{m}$) are released in the gas flow. In table I, we report the relation between particle diameters and characteristic response times, based on the definition given in Eq. (1). The numerical integration of the Langevin equations describing the particle phase is fully described in a recent paper⁴⁰. To compute the deposition velocity, we evaluate

F , the fraction of particles remaining in the flow, as a function of the axial position x ¹⁸. F is calculated by counting the number of particles that reach the sampling cross-section and it is defined by

$$F = \frac{\text{number of crossing particles}}{\text{total number of released particles}}$$

The particle deposition velocity is then computed as follows¹⁸

$$k_p = \frac{U_f d_t}{4(x_2 - x_1)} \ln \frac{F_1}{F_2} , \quad (21)$$

where d_t is the diameter of the pipe and F_i is particle fraction value at the $i - th$ sampling section. As previously explained, pure-deposition boundary conditions are applied for the particles, that is particles touching the wall are considered as being deposited and are removed from the domain. For the test-case simulated in this work, the aerosol flow is considered as dilute and, thus, interactions between turbulence and particles are only one-way.

A. Mean fluid value predictions

Although the purpose of this work is to analyse Lagrangian modeling for particle deposition, we first show some Eulerian results for the sake of completeness. Indeed, in the hybrid approach, the first step to be carried out is to evaluate the mean fluid variables which are included in the Lagrangian model, see eqs. (6)-(8). The pipe test-case considered in this work has been solved on an unstructured grid composed by 168000 points, that is $12 \times 28 \times 500$ points in the three directions. For all computations, we have used the Reynolds Averaged Navier Stokes (RANS) free code “Saturne”, which is an in-house code developed at Electricité de France. All details about this rather classical computational fluid dynamics code can be found elsewhere⁴¹. Grid-independence has been assured, as shown in fig. 1a. Wall-boundary conditions have been imposed through classical wall-functions, with the first grid-point put at $y^+ \approx 50$ ⁴². At the inlet, the mean velocity is imposed uniform and equal to the bulk velocity U_m given by Reynolds number $Re = \frac{U_m H}{\nu}$, where H is the Pipe diam-

eter. No variation with radial position is present. Steady state was obtained after some downstream distance; nevertheless, in order to be sure that inlet conditions have no effect on our results, only second half of the channel has been considered. Outflow conditions were imposed at the outlet.

Standard $k - \epsilon$ and R_{ij} turbulence models have been used. Results are in line with the known performance of these models in wall flows and very similar results have been obtained with both models. In fig.1a, the mean velocity in the axial direction obtained with both models for two grids are shown and compared against analytical results⁴³, which fit very well DNS results of comparable Reynolds number⁴⁴. In fig.1b, the turbulent energy obtained with both models is shown.

B. Results with the standard model

First of all, numerical tests have been performed to check that the results were independent of the values of numerical parameters, in particular the number of particles and the time-step. Results are shown in Fig. 2, where a standard $k - \epsilon$ turbulence model was applied for the fluid in the Eulerian solver. It is seen that numerical independence with respect of the time step is reached for the two numerical schemes (of order 1 and order 2), and that the influence of the order of convergence of the schemes is negligible. Based on these results, a time-step of $\Delta t = 10^{-4}s$ was chosen for the different calculations, while keeping the second-order algorithm. The independence of the deposition velocity with respect to the time-step illustrates that the numerical scheme is stable for the whole range of particles. It is well known⁹ that, for a given time step, the stochastic equations for turbulent particle become stiff for small diameters and near the wall. If this mathematical characteristic is not well addressed with an appropriate numerical scheme, the stiffness problem imposes the use of very small time-step in order to prevent the presence of numerical instabilities^{18,19} which may also lead to the use of an unphysical time-step. Thus, the present algorithm appears as satisfactory for particle deposition computations.

Apart from numerical errors due to the time-accuracy of the numerical scheme, an analysis of the statistical error has been carried out. Since particle deposition velocities are calculated by a Monte Carlo method, it is important to check that the number of particles (which represents samples of the pdf) is sufficiently high so that statistical error is limited. In Fig. 2, we present also results obtained with three different values of N , which is the number of particles used for each class of diameter : $N = 500, 1000$ and 5000 . As it appears, although results change very slightly with increasing N , there is no clear difference between these results and it seems that 500 particles for each class of diameter is already high enough. However, we have chosen for further simulations the value of $N = 1000$ particles for each class of diameter, in order to reduce statistical noise.

In figure 3, results obtained with the standard PDF model, Eqs. (6)-(8), can be compared with experimental data. Two different turbulent models for the simulation of the continuous phase were used, namely the standard $k - \epsilon$ and $R_{ij} - \epsilon$ models, both with wall-function boundary conditions. The difference between the simulations performed with the two different turbulence models is negligible. This is not too surprising, since in this test-case the two models give similar mean fluid profiles, as shown in previous section. These results are coherent with those obtained in an analogous configuration by Schuen⁴⁷.

It is possible to divide the results in two main categories. For heavy particles ($\tau_p^+ > 10$), the model prediction agrees very well with experiments. On the contrary, for light particles ($\tau_p^+ < 10$), the deposition velocities remain at the same level as for heavy particles, and are therefore strongly overestimated. This fact shows that the stochastic model proposed, in its standard form, is not suitable to simulate deposition phenomena in this range. In particular, there is no appreciable difference between the two categories ($\tau_p^+ < 10$ and $\tau_p^+ > 10$) in the standard form of the model, while in reality deposition velocity diminishes by three order of magnitude.

This seems to be in line with experimental and DNS results, heavy particles are not much affected by near-wall boundary layer and by the specific features of the instantaneous turbulent structures and, thus, the general model provides an adequate description. On the

contrary, for light particles, the physical mechanism of deposition changes, with a growing importance of turbulent structures and near-wall physics in general. The standard form of the PDF model is not sensitive to this change, giving for particles in the whole spectrum of diameters almost the same results.

C. Influence of mean fluid profiles

As previously mentioned, in the standard form of the PDF model, the fluid boundary layer is simulated with the wall-function approach. This method assures a reasonable approximate mean fluid profile in the logarithmic region without solving explicitly the viscous sub-layer. Nevertheless, given that the results obtained with the standard model are not satisfying, a question arises : is the prediction of particle deposition velocity sensitive to changes in the fluid mean fields ? Or, to be more precise, can we improve predictions by changing the value of mean-quantity profiles and of parameters (such as T_L) that enter in the Langevin equation, while keeping the same form of the model?

The influence of such approximations was recently investigated by other Lagrangian models¹⁸. Following the same reasoning, we have carried out simulations where the computed mean fluid fields are replaced by given ones in the whole domain and, consequently, wall-function boundary conditions are suppressed. In the chosen test-case, analytical solutions for the mean fluid fields ($\langle \mathbf{U} \rangle, k, \langle \epsilon \rangle$) can be found⁴³ and DNS data are also available for the entire region of simulation. It is important to underline that, for this particular numerical study, grid resolution has been largely improved, with a grid spacing near-to-the-wall of $\Delta y^+ \approx 1$. This should assure that mean variations are captured with sufficient detail. The aim of this substitution is to make a sensitivity analysis of the standard model with respect to mean fluid quantities, because one might expect that smaller particles are more sensitive to the rapid variations of mean quantities expected in near-wall layer. In figure 4, we present results for different tests. A first sensitivity test has been carried out with imposing the axial mean fluid velocity given by the law-of-the-wall equations $\langle U_{f,i} \rangle = u^+$, that is we have used

the theoretical analytical value for this variable. In the second test, again the mean fluid velocity has been computed through this law, but we have also used turbulent kinetic energy (k) and turbulent dissipation rate (ϵ) curve-fitted to the DNS data¹⁸, thus all mean fluid profiles used in this test are “exact”, in the sense that they are either given by the analytical solution (mean velocity) or by DNS simulations.

The influence of the fluid mean profiles on the predicted values is limited and the model does not appear to be sensitive to them. The deposition rate remains over-predicted by the model for light particles. This may be explained by the fact that the effect of the new mean fluid profiles is concentrated in a thin region. Most important quantities are expected to be the turbulent kinetic energy and the wall-normal stress³⁹. Nevertheless, turbulent kinetic energy decreases only from $y^+ \approx 10$, where it reaches its maximum in correspondence with peak production. Wall-normal stress peaks further but yet near-to-the-wall, at about $y^+ \approx 50$ ⁴⁵. The resulting effect is not easy to be foreseen and it may be negligible with respect to the overall effect of migration of particles towards the wall due to the net mean flow. In order to further support this argument, we have computed the mean near-wall residence time (in the layer $y^+ < 30$) of deposited particles, for each class of diameters. We have chosen to monitor the particle residence-time because this quantity has been found to properly distinguish different deposition mechanisms¹³. In Table II, the results obtained for each class of diameters are given for the simulation with all exact fluid profiles. For the sake of clarity, the residence time is always expressed in nondimensional wall- units (i.e. normalized using the kinematic viscosity and the friction velocity). In the model, all particles, regardless of their diameter, are found as depositing by the free-flight mechanism, that is with a small near-wall residence time. Furthermore, the residence time grows slightly with diameters. This fact shows that particles are dominated by the migratory flux and light particles are even faster than the biggest ones to reach walls, since the acceleration on particles is proportional to the inverse of diameter.

A first conclusion can be drawn: in the absence of a representation of turbulent coherent structures which can trap particles in the near-wall region and which describe correctly the

mechanisms of deposition, the mean fluid profiles are not found to be a significant factor. In some previous works^{18,39,46}, it was experienced that the introduction of exact mean fluid quantities improved the performance of discrete Lagrangian models. However, the same tendency has not been observed in the present work. With respect to this point, it may be worth remembering that the attention in these works was mainly devoted to the analysis of the Eulerian part of the hybrid approach and that, very often, a standard “random-walk” model was used for the Lagrangian part. In the present work, a rather complementary point of view has been followed, where the emphasis was put on the Lagrangian model and, more specifically, on the consistency between the Eulerian and Lagrangian formulations in the fluid limit. The theoretical issues related to this consistency question have already been developed in the previous part but they are further compounded by similar numerical issues, so that we believe that it is important to address carefully several aspects in practical computations while testing the sensitivity to mean fluid profiles :

- (a) Lagrangian models can be affected by spurious drifts^{20,17,32}, as discussed in the previous section, which may correspond to an artificial force which pushes small particles away from wall. It must be ensured that a correct mean pressure-gradient is correctly introduced before pursuing further tests³⁸.
- (b) Lagrangian models are written as stochastic differential equations (SDE) whose numerical integration is more subtle than classical ordinary differential equations (ODE). A straightforward approach based upon classical numerical schemes for ODE can lead also to the existence of spurious drifts, now of numerical origin^{9,48}.
- (c) In Lagrangian simulations, if standard numerical schemes are used, a very small time-step is required near the wall to guarantee numerical stability. This may lead to an unphysical behaviour, since present stochastic models are based upon the hypothesis that the time-step is much greater than the Kolmogorov time-scale $\Delta t \gg \tau_\eta$.
- (d) It has been found that it is important to ensure that the turbulence Eulerian model

and the Lagrangian one are as consistent as possible^{38,49}. The lack of consistency may also lead to unphysical results, at least for the limit case of very small particles³⁸. In particular, even with the exact mean profiles, the present Langevin model do not reproduce exactly the Reynolds stress, for example the wall-normal stress may be slightly underestimated, and thus this can limit the effect of the introduction of better Eulerian predictions.

With the previous issues in mind and given the results obtained in this section, we propose to retain the present Langevin model, but to implement it with a simple phenomenological model to account for some of the near-wall physical mechanisms due to coherent structures. The purpose of this new phenomenological model is two-fold: first to improve the model predictions in a ad-hoc but simple manner and, second, to investigate whether modeling more explicitly particle interactions with near-wall coherent structures is a direction worth pursuing.

D. Phenomenological model for coherent structures

The turbulent near-wall structures have been found to have a main role on the mechanism of particle deposition^{11,13}. For our purpose, the most interesting aspect is that depositing particles can be divided into two categories. In the first one, particles with large wall-normal velocity and small near-wall residence time, deposit mainly by the *free-flight* mechanism. In the second one, for particles with negligible wall-normal velocity and large near-wall residence time, the *diffusional* mechanism is the most important one.

More specifically, for light particles ($\tau_p^+ < 10$) the *diffusional* mechanism is shown to represent the sole mechanism useful to deposition, while its importance decreases as particles become heavier. Yet, Narayanan et al.¹³ show that the diffusional deposition mechanism still remains quantitatively important for heavy particles, at least in the intermediate range which is considered there. For example, for particles with $\tau_p^+ = 15$, only about 40 % of the particles are expected to deposit by the free-flight mechanism. However, for very heavy

particles ($\tau_p^+ \gg 10$) the *free-flight* mechanism is expected to become the dominant one. From a physical point of view, the different behavior between particles of different inertia can be explained in terms of the interaction with coherent structures in the near-wall region, notably with sweeps and ejections. Light particles remain trapped for a long time by these structures in a thin region ($y^+ < 3$) and deposit only by diffusion. Heavy particles, with a high enough wall-normal velocity, go through this region without being influenced and deposit after a small residence time.

Although diffusional deposition was found to be still important in the small range of diameters analyzed in DNS simulations, we can propose the following picture : heavy particles ($\tau_p^+ > 10$) deposit by the *free-flight* mechanism, while light particles ($\tau_p^+ < 10$) deposit by the *diffusional* mechanism. Though this represents a rough approximation, it can be considered as reasonable for the construction of a simple model. In effect, with our standard PDF model, heavy particles ($\tau_p^+ > 10$) are well treated, see Fig. 3. Therefore, for particles with ($\tau_p^+ > 10$) we do not need any model modification. For light particles the situation is completely different. Evidently, some instantaneous features of coherent structures are not well represented in our standard PDF model, so the idea is to add the main effects by new *ad-hoc* terms.

The results obtained by recent DNS computations suggest that the residence time of particles in near-wall region represents the most important parameter. Given this, we propose a simple phenomenological model which covers the whole range of diameter (heavy and light particles). The model introduces the notion of a residence time scale in the near-wall region for each class of diameter, say $T_s(d_p)$. The characteristic time scale $T_s(d)$ is function of particle diameters, and we propose to model it with the simple form

$$T_s = T_0 \exp \left(-\frac{d_p}{D_0} \right) . \quad (22)$$

This form is based on the dimensional guess $\frac{dT_s}{dd_p} = -T_s/D_0$ and it is chosen because it gives the good monotonic and asymptotic behavior. The two parameters D_0 and T_0 , not a priori known, can be extracted from the two values investigated by DNS ($\tau_p^+ = 5$ and $\tau_p^+ = 15$).

Although DNS gives only the statistical distribution of this quantity and not a single value, it is possible to roughly deduce from DNS results a mean value of $T_s^+ \sim 10^3$, for $\tau_p^+ = 5$, and $T_s^+ \sim 10^2$, for $\tau_p^+ = 15$. On the basis of these results, the parameter are evaluated to be $T_0^+ = 700$, $D_0^+ = 2.3 \times 10^{-4}$ in adimensional wall units. Though these results have been deduced from a single DNS computation at a given Reynolds-number, they are computed from adimensional quantities related to wall ones, which are known to have almost universal character³⁴, and the present estimates are assumed to have some general validity.

Since our model is aimed at introducing features of coherent structures whose influence is limited to a thin region near the wall¹³, it seems reasonable to apply it in the numerical simulations by imposing *ad-hoc* boundary conditions : when a particle hits a wall, it deposits only if its residence time in the near-wall region (defined as the zone $y^+ < 30$) is greater than T_s . Otherwise, it remains at the wall and its velocity is put to zero, but it can be reentrained and move again in the flow. These boundary conditions are applied to each class of particle diameters.

To sum up, the complete Langevin PDF model proposed is as follows

$$\left. \begin{aligned} dx_{p,i} &= U_{p,i} dt \\ dU_{p,i} &= \frac{1}{\tau_p} (U_{s,i} - U_{p,i}) dt \\ dU_{s,i} &= A_{s,i}(t, \mathbf{Z}) dt + B_{s,ij}(t, \mathbf{Z}) dW_j. \end{aligned} \right\} \text{SDE model} \quad (23)$$

$$\left. \begin{aligned} &\text{Particle deposition ; if } T_p > T_s \\ &U_{p,i} = 0, \quad x_{p,i} = 0 ; \text{ if } T_p < T_s \end{aligned} \right\} \text{Particle B.C.} \quad (24)$$

where T_p represents the residence time of the given particle in the near-wall layer $y^+ < 30$.

In our picture, heavy particles ($\tau_p^+ > 10$) deposit each time they reach the wall, since the residence time scale tends to zero rapidly with particle diameter. On the other hand, light particles ($\tau_p^+ < 10$) deposit only if they remain in the near-wall region for a sufficient time.

In Fig. 5, the results obtained with the new model are represented by the curve indicated by $f(TS)$. A good agreement with experimental data is retrieved, and in particular the sharp decrease of the deposition velocity for light particles is correctly reproduced. In the same

figure, we present also a second curve indicated by $f(TS/2)$, which represents the results obtained by using in the model a residence time scale equal to $T_s/2$. These results indicate that the dependence on the residence time is critical for lighter particles. In fact, in this particular test-case considered it represents the main effect.

In Fig. 6, we present the curve representing the fraction of particles remaining in the flow versus pipe axis for the two functions of the characteristic time scale used, that is T_s and $T_s/2$. For reasons of clarity, in the figure we show only 4 classes of diameters, which, however, represent all the regimes. The figure shows again that, for small and intermediate diameters, there is a noticeable difference in the fraction of particles which deposit, while for large particles the behavior is very similar.

In order to further assess the model function given by Eq. (22) we show, in Fig. 7, the number of particles which deposit for each class of diameters, in the case of the function T_s . We computed the fraction of particles deposited by the free-flight mechanism, and the fraction of particles depositing by the diffusional one. We can see that the model reproduces reasonably well the physical behavior proposed by DNS calculations. The diffusional mechanism is the most important for small particles ($\tau_p^+ < 10$), while for the other classes free-flight mechanism becomes the only efficient one. Moreover, the proportion between the two mechanisms is correctly given, at least for light particles. For the class of diameter $\tau_p^+ = 6.4$, 80% of particles are found to deposit by diffusional mechanism, while DNS results indicate a rate of 90% for $\tau_p^+ = 5$. Finally, it is worth noting that the Lagrangian approach proposed in this work is grid-independent and valid for nominally infinite Reynolds-number, thus should be easily used in much more complex geometries and grids.

IV. CONCLUSIONS

In this paper we have presented a numerical study of particle deposition in a turbulent pipe flow using a Langevin PDF model recently proposed²¹. In its standard formulation, the model has been found to be unable to reproduce the correct deposition velocity for light

particles ($\tau_p^+ < 10$). Indeed, results obtained with the standard form of the model have revealed a deposition velocity which is only slightly sensitive to particle inertia. Moreover, sensitivity tests have indicated that this outcome is not noticeably modified when mean fluid profiles are changed. As a simple and first step toward considering the specific effects of coherent structures, a new phenomenological model, built on the basis of DNS results, has been proposed and introduced in the numerical simulations. The results obtained with this model are in good agreement with experiments and show that:

- (i) One way to improve significantly the statistical description of particle deposition is to take into account some geometrical features of the flow, through the sweeps and ejections events. In particular, residence-time in the near-wall region¹³ which reflects their influence can be considered as a relevant parameter.
- (ii) This model represents already a first attempt to relate a statistical description of the flow with a geometrical one, because we have put (crudely) some geometrical features of the instantaneous flow (coherent structures) in the framework of a statistical flow description, such as the present Langevin model. This first proposition opens the road for a more systematic introduction of geometrical features in statistical PDF approach, where coherent structures in wall-bounded flows could be introduced as new stochastic terms in the modeled equations. Given present results, this more explicit and rigorous stochastic approach appears as a good candidate for the construction of particle deposition models based on physical principles. This is the subject of current research and of new stochastic models^{50,51}.
- (iii) Even in its present formulation, the Langevin model proposed here yields satisfactory results and can be attractive for engineering applications, given its simplicity and stability (large time-steps can be used in the whole domain and for the whole range of particle diameter).

V. ACKNOWLEDGMENTS

S. Chibbaro's work is supported by a ERG EU grant. This work makes use of results produced by the PI2S2 Project managed by the Consorzio COMETA, a project co-funded by the Italian Ministry of University and Research (MIUR). More information is available at <http://www.pi2s2.it> and <http://www.consorzio-cometa.it>. he greatly acknowledges the financial support given also by the consortium SCIRE. We greatly acknowledge the important help of M. Ouraou for the fluid numerical computations. Moreover, S. Chibbaro would like to express special thanks to M. Ouraou for his constant, patient and friendly support in all computational aspects during his stay at EDF.

REFERENCES

- ¹ B. Liu and K. Agarwal, “Experimental observation of aerosol deposition in turbulent flow”, *Aerosol Science*, **5**, 145 (1974).
- ² D.D. McCoy and T.J. Hanratty, “Rate of deposition of droplets in annular two-phase flow”, *Int. J. Multiphase Flow*, **3**, 319 (1977).
- ³ J.K. Eaton and J.R. Fessler, “Preferential concentration of particles by turbulence”, *Int. J. Multiphase Flow*, **20**, 169 (1994).
- ⁴ D. Kaftori, G. Hestroni and S. Banerjee, “Particle behavior in the turbulence boundary layer. I Motion, deposition and entrainment”, *Phys. Fluids*, **7**, 1095 (1995).
- ⁵ D. Kaftori, G. Hestroni and S. Banerjee, “Particle behavior in the turbulence boundary layer. II Velocity and distribution profiles”, *Phys. Fluids*, **7**, 1107 (1995).
- ⁶ J. B. McLaughlin, “Aerosol particle deposition in numerically simulated channel flow”, *Phys. Fluids A* **1**, 1211 (1989).
- ⁷ J.W. Brooke, K. Kontomaris, T.J. Hanratty and J.B. McLaughlin, “Turbulent deposition and trapping of aerosols at a wall”, *Phys. Fluids A*, **4**, 825 (1992).
- ⁸ D. W. Rouson and J.K. Eaton “On the preferential concentration of solid particles in turbulent channel flow”, *J. Fluid Mech.* **428**, 149 (2001).
- ⁹ E. Peirano, S. Chibbaro, J. Pozorski and J.P. Minier “Mean-Field/PDF Numerical approach for polydispersed turbulent two-phase flows”, *Progress in Energy and Combustion Sciences*, **32**, 315 (2006).
- ¹⁰ K. Friedlander and H.F. Johnstone, “Deposition of suspended particles from turbulent gas streams”, *Ind. Eng. Chem.* **49**, 1151 (1957).
- ¹¹ C. Marchioli and A. Soldati, “Mechanisms for particle transfer and segregation in a turbulent boundary layer”, *J. Fluid Mech.*, **468**, 283 (2002).

- ¹² C. Marchioli, A. Giusti, M.V. Salvetti and A. Soldati, “A direct numerical simulations of particle wall transfer in upward turbulent pipe flow”, *International journal of Multiphase flow*, **29**, 1017 (2003).
- ¹³ C. Narayanan, D. Lakehal, L. Botto and A. Soldati, “Mechanisms of particle deposition in a fully developed turbulent open channel flow”, *Phys. Fluids*, **3**, 763 (2003).
- ¹⁴ M. Picciotto, C. Marchioli and A. Soldati, “Characterization of near-wall accumulation regions for inertial particles in turbulent boundary layers”, *Phys. Fluids*, **17**, 098101 (2005).
- ¹⁵ P. K. Yeung and S. B. Pope, “Lagrangian statistics from direct numerical simulations of isotropic turbulence”, *J. Fluid Mech.*, **207**, 531 (1989).
- ¹⁶ B. Van Harlem, B.J. Boersma and F.T.M. Nieuwstadt, “Direct numerical simulation of particle deposition onto a free-slip and no-slip surface”, *Phys. Fluids*, **10**, 2608 (1998).
- ¹⁷ J.M. MacInnes and F.V. Bracco, “Stochastic particle dispersion modeling and the tracer-particle limit”, *Phys. Fluids A*, **4**, 2809 (1992).
- ¹⁸ E.A. Matida, K. Nishino and K. Torii, “Statistical simulation of particle deposition on the wall from turbulent dispersed pipe flow”, *International Journal of Heat and Fluid Flow*, **21**, 389 (2000).
- ¹⁹ C. Kroger and Y. Drossinos, “A random-walk simulation of thermophoretic particle deposition in a turbulent boundary layer”, *Int. J. Multiphase Flow*, **26**, 1325 (2000).
- ²⁰ S. B. Pope, “Consistency conditions for random-walk models of turbulent dispersion”, *Phys. Fluids*, **30**, 2374 (1987).
- ²¹ J.P. Minier, E. Peirano and S. Chibbaro, “PDF model based on Langevin equation for polydispersed two-phase flows applied to a bluff-body gas-solid flow”, *Phys. Fluids* **16**, 2419 (2004).
- ²² M.R. Maxey, and J.J. Riley, “Equation of Motion for a Small Rigid Sphere in a Nonuniform

- Flow”, *Phys. Fluids* **26**, 883 (1983).
- ²³ R. Gatignol, “The Faxén formulae for a rigid particle in an unsteady non-uniform Stokes flow”, *Journal de Mécanique Théorique et Appliquée*, **1**, 143 (1983).
- ²⁴ R. Clift, J. R. Grace, and M. E. Weber, *Bubbles, Drops and Particles*. Academic Press. New York, 1978.
- ²⁵ J.B. McLaughlin, “Inertial migration of a small sphere in linear shear flows”, *J. Fluid Mech.*, **224**, 261 (1991).
- ²⁶ J.B. McLaughlin, “The lift on a small sphere in wall-bounded linear shear flows”, *J. Fluid Mech.*, **246**, 249 (1993).
- ²⁷ J.B. McLaughlin, “Numerical computation of particle-turbulence interaction”, *Int. J. Multiphase Flow*, **20**, 211 (1994).
- ²⁸ Q. Wang, K.D. Squires, M. Chen and J.B. McLaughlin, “On the role of the lift force in turbulence simulations of particle deposition”, *Int. J. Multiphase Flow*, **23**, 749 (1997).
- ²⁹ I. Zahmatkesh , “On the importance of thermophoresis and brownian diffusion for the deposition of micro- and nanoparticles ”, *Int. Journal of heat and mass transfer* **35**, 369 (2008).
- ³⁰ C.-L. Chen, and K.-C. Chan , “Combined effects of thermophoresis and electrophoresis on particle deposition onto a wavy surface disk”, *Int. Journal of heat and mass transfer* in press.
- ³¹ J. Israelachvili *Intermolecular and surface forces*. Academic Press, England 1991.
- ³² J.P. Minier and E. Peirano , “The PDF approach to turbulent polydispersed two-phase flows ”, *Phys. Reports* **352**, 1 (2001).
- ³³ S. B. Pope, “Lagrangian pdf methods for turbulent reactive flows”, *Ann. Rev. Fluid Mech.*, **26**, 23 (1994).

- ³⁴ S.B. Pope. *Turbulent Flows*. Cambridge University Press, Cambridge 2000.
- ³⁵ S. B. Pope, “On the Relationship between Stochastic Lagrangian Models of Turbulence and Second-Order Closures”, *Phys. Fluids*, **6**, 973 (1994).
- ³⁶ J.P. Minier and J. Pozorski, “Wall-boundary conditions in probability density function methods and application to a turbulent channel flow”, *Phys. Fluids* **11**, 9, 2632 (1999).
- ³⁷ M. Wacawczyk, J. Pozorski and J-P. Minier “Probability density function computation of turbulent flows with a new near-wall model”, *Phys. Fluids*, **16**, 1410 (2004).
- ³⁸ S. Chibbaro, and J.-P. Minier “Langevin and hybrid models for two-phase flow simulations”, *EDF Tech. rep.*, H-I81-2007-02166 (2007).
- ³⁹ S. Parker, T. Foat, and S. Preston “Towards quantitative prediction of aerosol deposition from turbulent flows”, *Journal of Aerosol Science*, **39**, 99 (2008).
- ⁴⁰ J-P. Minier, E. Peirano and S. Chibbaro, “Weak first- and second-order numerical schemes for stochastic differential equations appearing in Lagrangian two-phase flow modeling”. *Monte Carlo Meth. and Appl.*, **9**, 93 (2003).
- ⁴¹ Archambeau and et al. “Guide pratique d’utilisation de Code_Saturne version 1.2”, *EDF Technical report*, HI-83/05/036 (2005).
- ⁴² D.C. Wilcox “Turbulence modeling for CFD”, DCW Industries, La Canada, USA (1993).
- ⁴³ A. S. Monin and A. M. Yaglom. *Statistical Fluid Mechanics*. MIT Press, Cambridge, Mass, 1975.
- ⁴⁴ N.N. Mansour, J. Kim, and P. Moin “Reynolds-stress and dissipation-rate budgets in a turbulent channel flow.”, *Journal of Fluid Mechanics*, **194**, 15 (1988).
- ⁴⁵ J. Kim, P. Moin, and R. Moser “Turbulence statistics in fully developed channel flow at low Reynolds number.”, *Journal of Fluid Mechanics*, **177**, 133 (1987).

- ⁴⁶ Y. Wang, and P.W. James “On the effect of anisotropy on the turbulent dispersion and deposition of small particles”, *Int. Journal of Multiphase flow*, **25**, 551 (1999).
- ⁴⁷ J.S. Schuen, L.D. Chen and G.M. Faeth, “Evaluation of a stochastic model of particle dispersion in a turbulent round jet”, *AIChE J.*, **29**, 167 (1987).
- ⁴⁸ J-P. Minier, R. Cao, S.B. Pope, Comment on the article “an effective particle tracing scheme on structured/unstructured grids in hybrid Finite Volume/PDF Monte Carlo methods” by Li and Modest. *J. Comput. Phys.*, **186**, 356 (2003).
- ⁴⁹ M. Muradoglu, P. Jenny, S. B. Pope, and D. A. Caughey “A Consistent Hybrid Finite Volume/Particle Method for the PDF Equations of Turbulent Reactive Flows”. *J. Comput. Phys.*, **154**, 342 (1999).
- ⁵⁰ M. Guingo and J-P. Minier “A stochastic model of coherent structures in boundary layers for the simulation of particle deposition in turbulent flows”, *ICMF proceedings*, Leipzig (2007).
- ⁵¹ M. Guingo and J-P. Minier “A stochastic model of coherent structures for particle deposition in turbulent flows”, submitted to *Phys. Fluids*, (2007).

TABLES

τ_p^+	Diameters (μm)
0.2	1.4
0.4	2.0
0.9	2.9
1.9	4.3
3.5	5.8
6.4	7.8
13.2	11.2
29.6	16.8
122.7	34.2
492.2	68.5

TABLE I. Relation between τ_p^+ and particle diameters.

τ_p^+	Diameters (μm)	Residence time (wall units)
0.2	1.4	29.5
0.4	2.0	29.9
0.9	2.9	28.7
1.9	4.3	30.9
3.5	5.8	31.5
6.4	7.8	31.6
13.2	11.2	35.4
29.6	16.8	40.6
122.7	34.2	55.3
492.2	68.5	96.8

TABLE II. Mean residence time for different classes of particle diameter in the case of exact mean fluid profiles, see $k^+ - \epsilon^+$ curve in Fig. 4.

List of Figures

- 1 (a): The mean velocity of the fluid phase is shown versus the distance from the wall. All quantities are made non-dimensional with the wall friction velocity and viscosity. 5 curves are shown: the ones labeled by “grid 1” represent the results obtained with the grid used throughout this paper (168000 cells) with both turbulence models used, namely $k - \epsilon$ and $R_{ij} - \epsilon$. The curves labelled “grid 2” are obtained on a grid with a resolution doubled in radial and azimuthal direction with both turbulence models. Results are very similar and therefore the grid-independence can be considered reached. The last curve shows the analytical curve that fits DNS results. (b): Adimensional turbulent kinetic energy is shown versus the adimensional distance from the wall. Analytical/DNS results are also shown for comparison. As expected, the peak of the kinetic energy is under-estimated by present turbulent models. Globally speaking, our numerical results are in line with standard performances of these models³⁴. 34
- 2 (a): Analysis of the convergence of the numerical scheme with the order and the time-step. The deposition velocity (y axis) is shown versus adimensional particle response time for different numerical configurations. For the test-case studied in this work, it is seen that for $\Delta t = 10^{-4}$ the results have reached the convergence and that the order of the scheme is not a key. (b): Analysis of the particle number influence on the results of deposition velocity. The Deposition velocity (y axis) is shown versus adimensional particle response time for some configurations with a different number of particles. It is seen that $N = 500$ is enough to guarantee the independence of the results from the number of particles used. 35

3	Analysis of the influence of the turbulence model used for the fluid phase. The deposition velocity obtained with different turbulent models is shown: $k - \epsilon$ circles, $R_{ij} - \epsilon$ squares. The results are almost indistinguishable, showing that the stochastic model used in this work for the description of the particle phase is not much affected by the turbulence model used for the computation of the mean fluid variables.	36
4	Deposition velocity with different fluid velocity profiles. Triangles down are the experimental value. Circles are obtained with all mean fluid quantities given by $k - \epsilon$ model (as in the previous picture). Diamond curve is obtained imposing axial mean fluid velocity given by the law-of-the-wall equations $\langle U_{f,i} \rangle = u^+$. For the result indicated by diamonds with $k^+ - \epsilon^+$, the mean fluid velocity is always given by the same law, and also turbulent kinetic energy (k) and turbulent dissipation rate (ϵ) are curve-fitted to the DNS data ¹⁸ , thus all mean fluid profiles are exact.	37
5	Deposition rate velocity for the different model used. In all numerical cases the continuous phase is solved via standard $k - \epsilon$ model. Experimental results are given for reference (triangle down). The standard results are indicated by the curve labeled with $k - \epsilon$ (circles). The results obtained with the new phenomenological model are shown by the curve indicated by k- ϵ f(TS) (crosses). In this case, particles can deposit only if they have remained in a small near-wall layer for a time given by the function f(TS), which is derived from DNS data. The last curve (stars) indicates the results obtained with the new phenomenological model but letting particles deposit even if they have remained only the half $T_s/2$ of the residence-time given by the function f(TS) derived from the DNS data. The results obtained with the phenomenological model with the residence-time computed through the function derived from DNS are in good agreement with experimental results, in particular small particles deposit only rarely.	38

6	Fraction of particles remaining airborne versus pipe length for different diameter classes. These results are obtained with the phenomenological model, as explained in fig. 5. Particles can deposit only after having stayed a certain residence-time in a small near-wall layer. The residence-time is different for each class of diameter and is computed for all classes through an empirical function $f(T_s)$ deducted from DNS data, which give the correct value only for two classes. In Fig (a), the results obtained using this function $f(T_s)$ derived from DNS data are shown. In Fig (b), results are shown the value of residence time given by $f(T_s)$ are divided by a factor two. It is seen that there is a little difference for the larger particles but that the difference is significant for the smaller. This indicates that the residence-time value used is crucial mainly for small particles.	39
7	Number of particles deposited for class of diameters and mechanism of deposition.	40

FIG

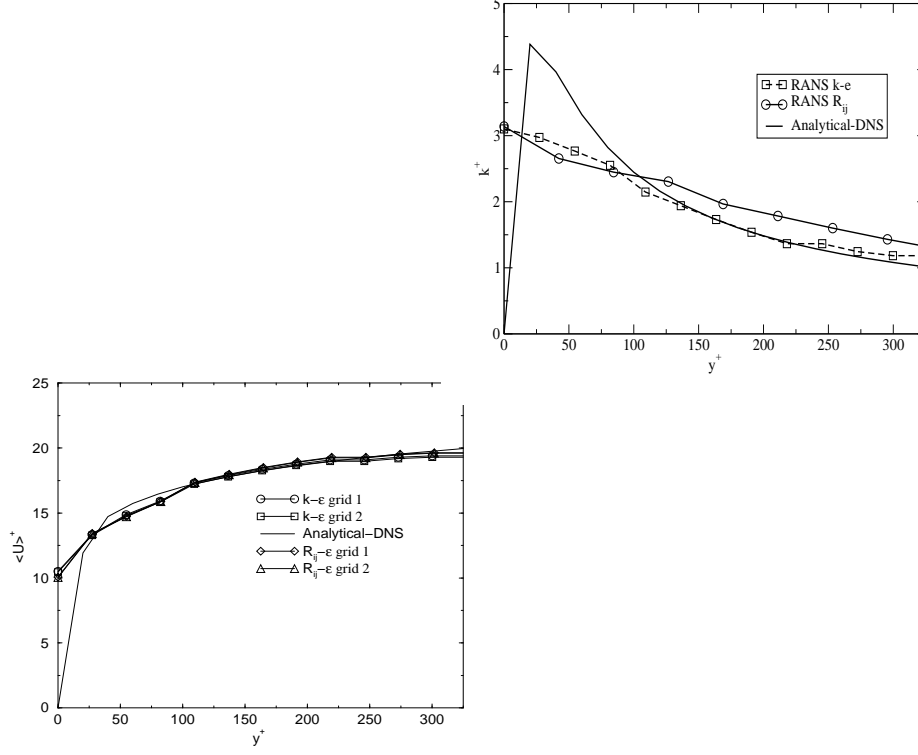


FIG. 1. (a): The mean velocity of the fluid phase is shown versus the distance from the wall. All quantities are made non-dimensional with the wall friction velocity and viscosity. 5 curves are shown: the ones labeled by “grid 1” represent the results obtained with the grid used throughout this paper (168000 cells) with both turbulence models used, namely $k - \epsilon$ and $R_{ij} - \epsilon$. The curves labelled “grid 2” are obtained on a grid with a resolution doubled in radial and azimuthal direction with both turbulence models. Results are very similar and therefore the grid-independence can be considered reached. The last curve shows the analytical curve that fits DNS results. (b): Dimensional turbulent kinetic energy is shown versus the adimensional distance from the wall. Analytical/DNS results are also shown for comparison. As expected, the peak of the kinetic energy is under-estimated by present turbulent models. Globally speaking, our numerical results are in line with standard performances of these models³⁴.

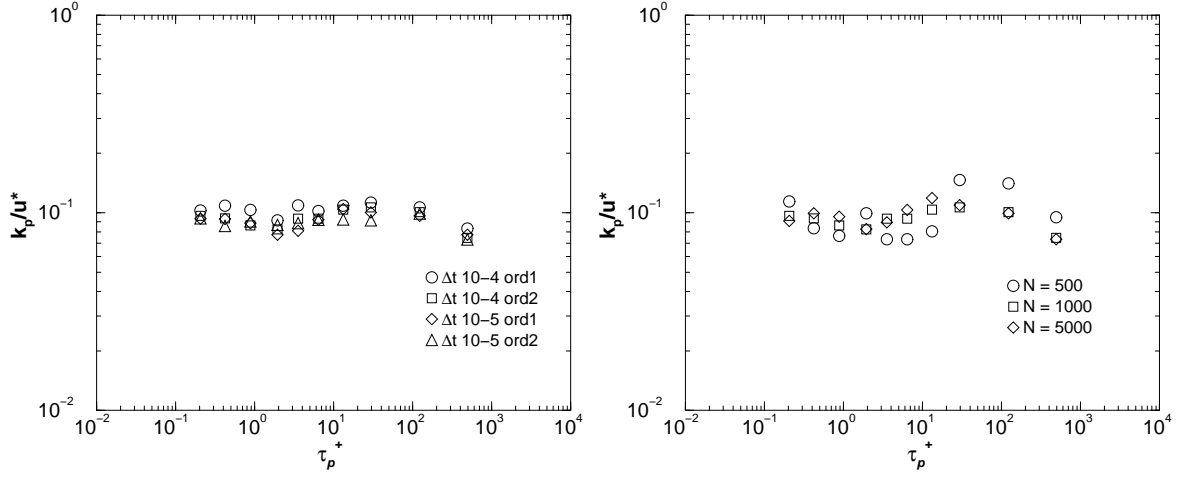


FIG. 2. (a): Analysis of the convergence of the numerical scheme with the order and the time-step. The deposition velocity (y axis) is shown versus adimensional particle response time for different numerical configurations. For the test-case studied in this work, it is seen that for $\Delta t = 10^{-4}$ the results have reached the convergence and that the order of the scheme is not a key. (b): Analysis of the particle number influence on the results of deposition velocity. The Deposition velocity (y axis) is shown versus adimensional particle response time for some configurations with a different number of particles. It is seen that $N = 500$ is enough to guarantee the independence of the results from the number of particles used.

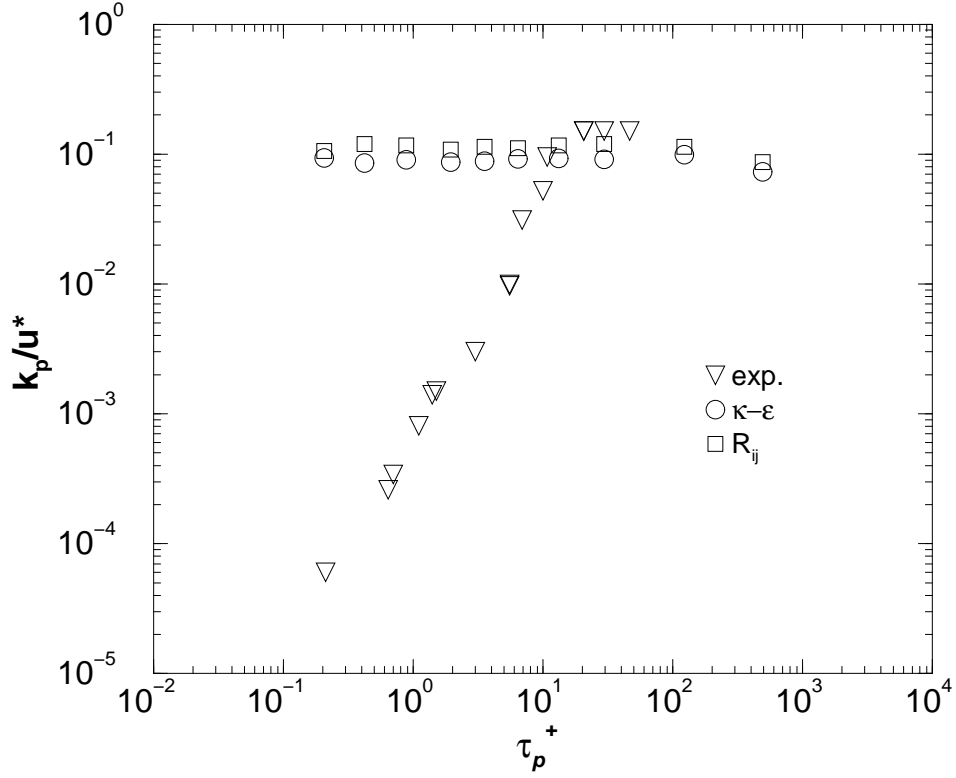


FIG. 3. Analysis of the influence of the turbulence model used for the fluid phase. The deposition velocity obtained with different turbulent models is shown: $k - \epsilon$ circles, $R_{ij} - \epsilon$ squares. The results are almost indistinguishable, showing that the stochastic model used in this work for the description of the particle phase is not much affected by the turbulence model used for the computation of the mean fluid variables.

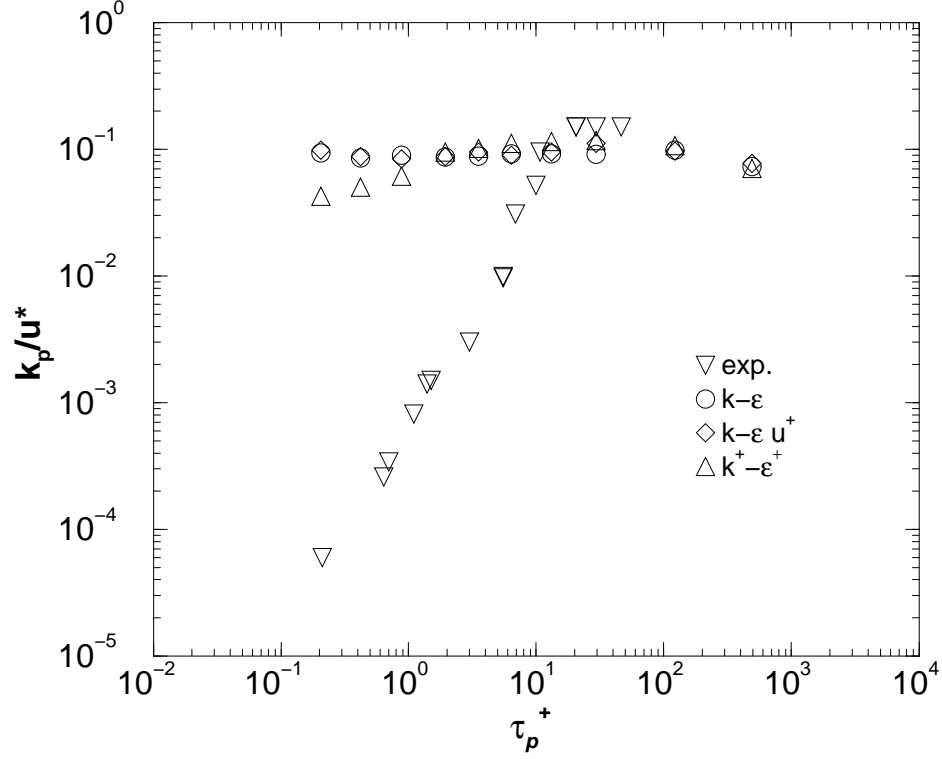


FIG. 4. Deposition velocity with different fluid velocity profiles. Triangles down are the experimental value. Circles are obtained with all mean fluid quantities given by $k - \epsilon$ model (as in the previous picture). Diamond curve is obtained imposing axial mean fluid velocity given by the law-of-the-wall equations $\langle U_{f,i} \rangle = u^+$. For the result indicated by diamonds with $k^+ - \epsilon^+$, the mean fluid velocity is always given by the same law, and also turbulent kinetic energy (k) and turbulent dissipation rate (ϵ) are curve-fitted to the DNS data¹⁸, thus all mean fluid profiles are exact.

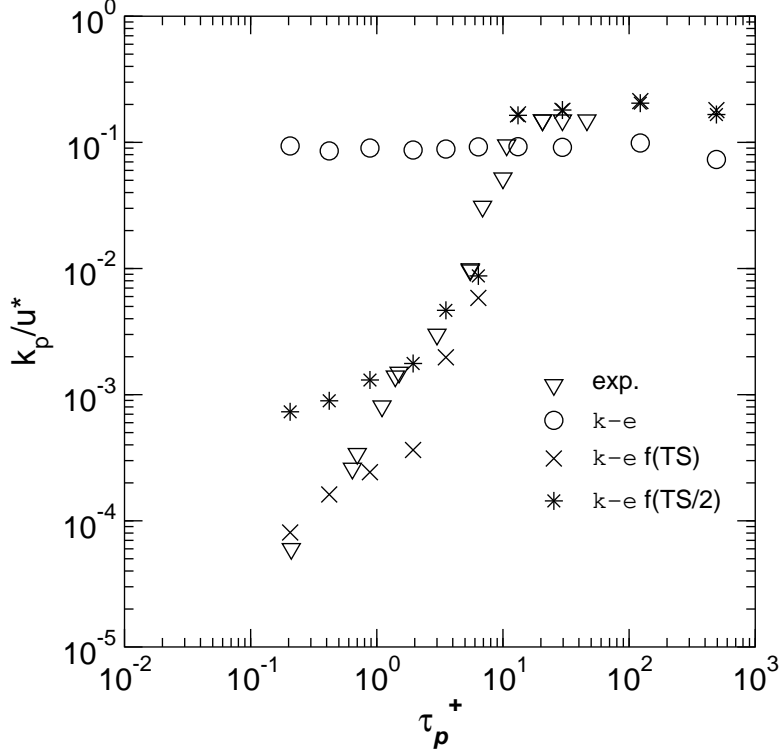


FIG. 5. Deposition rate velocity for the different model used. In all numerical cases the continuous phase is solved via standard $k - \epsilon$ model. Experimental results are given for reference (triangle down). The standard results are indicated by the curve labeled with $k - \epsilon$ (circles). The results obtained with the new phenomenological model are shown by the curve indicated by $k - \epsilon f(TS)$ (crosses). In this case, particles can deposit only if they have remained in a small near-wall layer for a time given by the function $f(TS)$, which is derived from DNS data. The last curve (stars) indicates the results obtained with the new phenomenological model but letting particles deposit even if they have remained only the half $T_s/2$ of the residence-time given by the function $f(TS)$ derived from the DNS data. The results obtained with the phenomenological model with the residence-time computed through the function derived from DNS are in good agreement with experimental results, in particular small particles deposit only rarely.

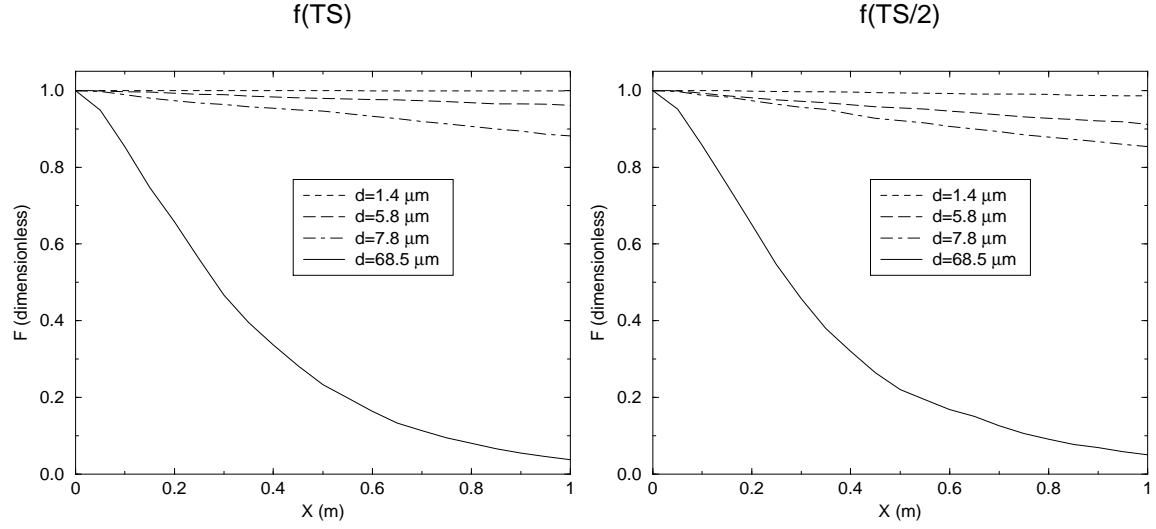


FIG. 6. Fraction of particles remaining airborne versus pipe length for different diameter classes.

These results are obtained with the phenomenological model, as explained in fig. 5. Particles can deposit only after having stayed a certain residence-time in a small near-wall layer. The residence-time is different for each class of diameter and is computed for all classes through an empirical function $f(Ts)$ deducted from DNS data, which give the correct value only for two classes. In Fig (a), the results obtained using this function $f(TS)$ derived from DNS data are shown. In Fig (b), results are shown the value of residence time given by $f(TS)$ are divided by a factor two. It is seen that there is a little difference for the larger particles but that the difference is significant for the smaller. This indicates that the residence-time value used is crucial mainly for small particles.

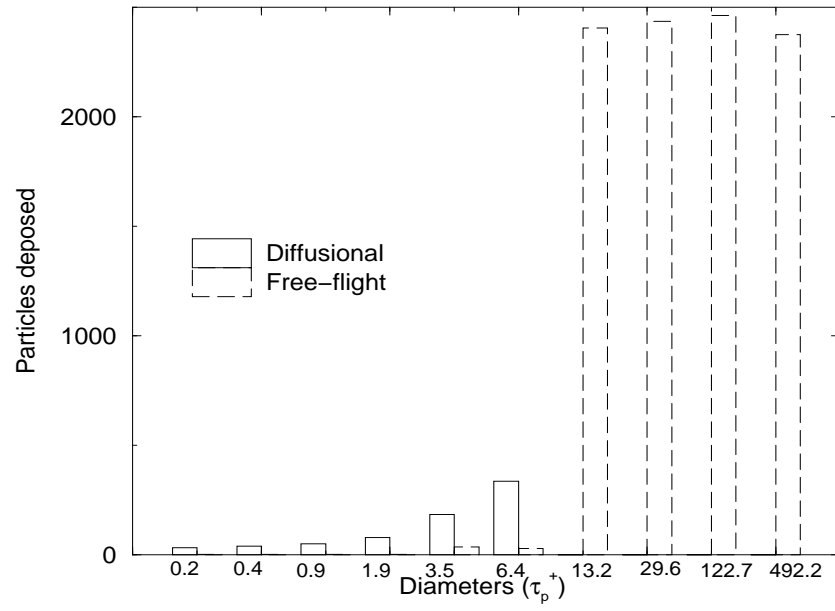


FIG. 7. Number of particles deposited for class of diameters and mechanism of deposition.